ANL/NSE-20/64

Development of Gamma Background Radiation Digital Twin with Machine Learning Algorithms

Application of Unsupervised Machine Learning to Detection of Anomalies and Nuisances in Gamma Background Radiation Environmental Screening Data

Nuclear Science and Engineering Division

ANL/NSE-20/64

Development of Gamma Background Radiation Digital Twin with Machine Learning Algorithms

Application of Unsupervised Machine Learning to Detection of Anomalies and Nuisances in Gamma Background Radiation Environmental Screening Data

prepared by
Allen Herrera[1,2], Eugene F. Moore, Alexander Heifetz[1]

[1]Nuclear Science Engineering Division, Argonne National Laboratory
[2]Department of Electrical and Computer Engineering, University of Texas at San Antonio
[3]Strategic Security Sciences, Argonne National Laboratory

November 1, 2020

Table of Contents

List of Figures

List of Tables

Abstract

Environmental screening of gamma radiation consists of detecting weak nuisance and anomaly signal in the presence of strong and highly varying background. In a typical scenario, a mobile detector-spectrometer continuously measures gamma radiation spectra in short, e.g., one-second, signal acquisition intervals. The measurement data is a 2D matrix, where one dimension is gamma ray energy, and the other dimension is the number of measurements or total time. In principle, gamma radiation sources can be detected and identified from the measured data by their unique spectral lines. Detecting sources from data measured in a search scenario is difficult due to the highly varying background because of naturally occurring radioactive material (NORM), and low signal-to-noise ratio (S/N) of spectral signal measured during one-second acquisition intervals. The objective of this work is to explore *unsupervised* machine learning (ML) algorithms for development of a *digital twin* of gamma radiation background, and for detection and identification of weak nuisances and anomalies events in the presence of highly fluctuating background.

In one segment of work, we developed a gamma background estimation model using a Long-short term memory (LSTM) network for one-step CPS time series prediction [4]. The LSTM model was validated with two data sets of measurements from two independent NaI detectors positioned on a mobile platform. The data sets contained background radiation only and no orphan isotope sources. The LSTM model was constructed and tested using data from one of the detectors. Performance of the LSTM model was validate through one-step prediction of CPS time series of *another* NaI detector *without re-training*. This approach allows to create a *digital twin* for nuclear background estimation. Using LSTM, it could be possible to detect a source through subtraction of the estimated counts from the measured background.

In another segment of work, we investigated detection of gamma emitting sources in the presence of complex background using unsupervised machine learning. Spectral lines of isotopes are difficult to observe in one-second measurements. Averaging over the entire measurement campaign data set reveals spectral lines of most common background isotopes. Spectral lines of orphan sources, which might appear only in a few measurements during the campaign, will be washed out if averaging is performed over the entire measurement data set. The approach we have explored consists of extracting one-second measurements containing weak spectral features through data clustering. Averaging one-second spectra in a cluster should reveal the presence of anomaly sources. We created two ML models using K-means clustering and Neural Network Self-organizing Map (SOM) [5,6]. Performance of these ML models was benchmarked using search data. One data set contained ^{137}Cs source, and another dataset contained ^{131}I source.

1. Introduction

Environmental screening of gamma radiation consists of detecting weak nuisance and anomaly signal in the presence of strong and highly varying background. In a typical scenario, a mobile detector-spectrometer continuously measures gamma radiation spectra in short, e.g., one-second, signal acquisition intervals. The measurement data is a 2D matrix, where one dimension is gamma ray energy, and the other dimension is the number of measurements or total time. In principle, gamma radiation sources can be detected and identified from the measured data by their unique spectral lines. Detecting sources from data measured in a search scenario is difficult due to the highly varying background because of naturally occurring radioactive material (NORM), and low signal-to-noise ratio (S/N) of spectral signal measured during one-second acquisition intervals. The objective of this work is to explore *unsupervised* machine learning (ML) algorithms for development of a *digital twin* of gamma radiation background, and for detection and identification of weak nuisances and anomalies events in the presence of highly fluctuating background.

As an example, Figure 1 shows images of gamma counts obtained with NaI detectors placed on a mobile platform in a drive through portions of the city of Chicago. Gamma counts per second (CPS), which are integrated over the energy spectrum, are displayed on the city map with pseudo color. Brighter counts indicate larger number of total counts.

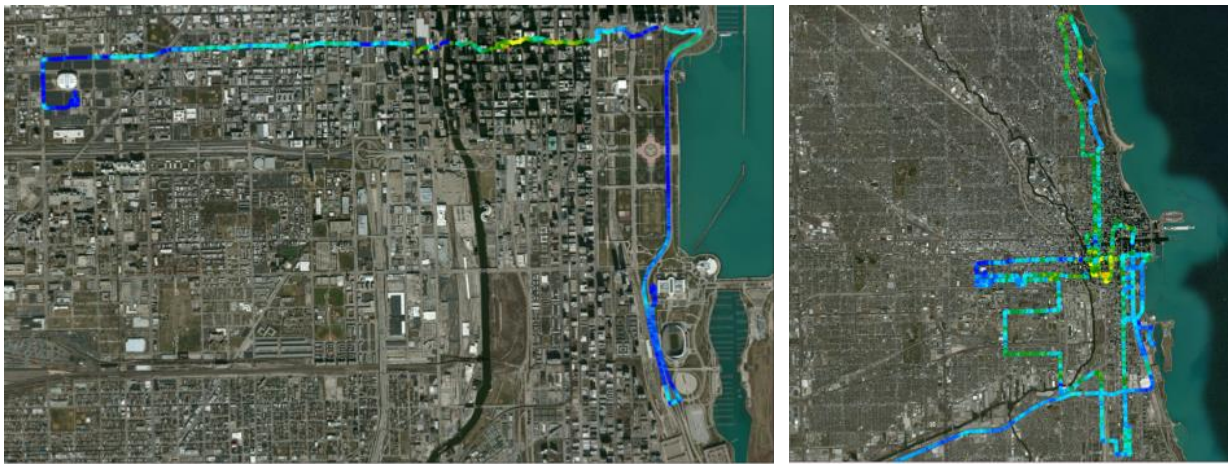

Figure 1 – Gamma counts, measured while driving with NaI detector through sections of the city of Chicago, displayed with pseudo color. Brighter colors indicate larger number of total counts.

Figure 2 shows the time series of gamma counts per second (CPS) measured during an environment screening campaign. As seen in the figure, there is significant fluctuation of gamma counts due to NORM in an urban setting.

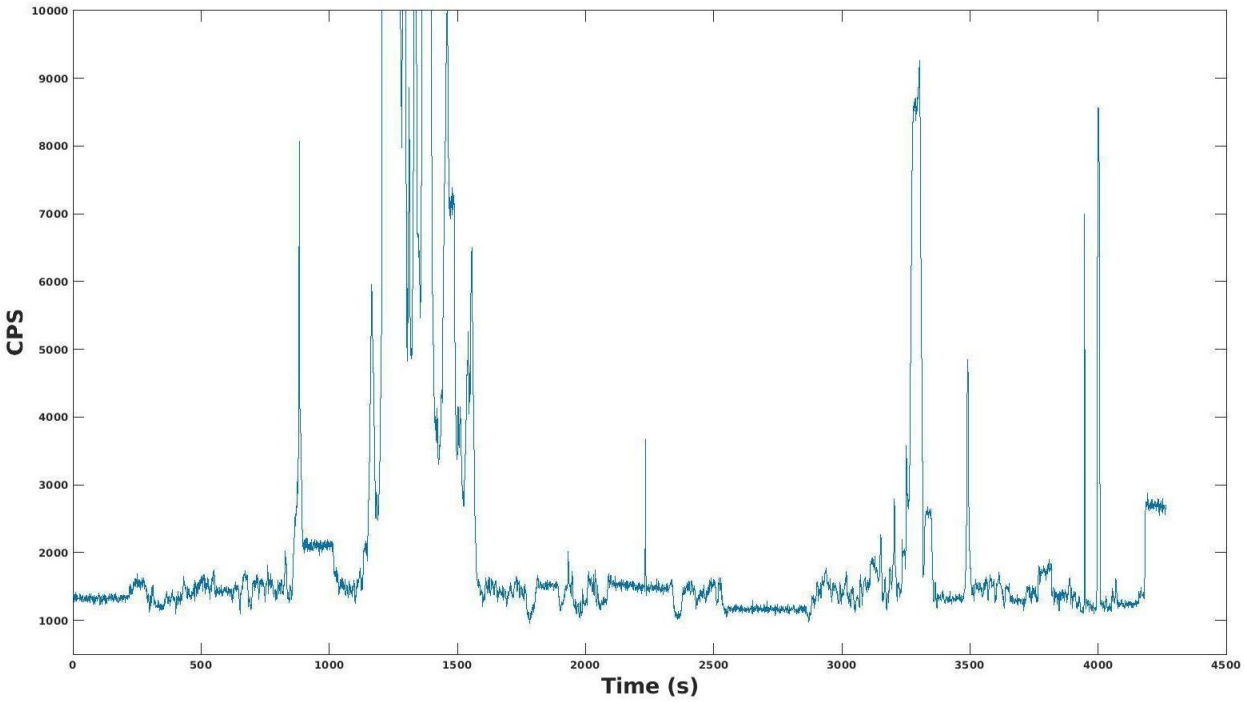

Figure 2 – Example of time dependence of total gamma counts per second (CPS). Fluctuations are primarily due to variation in NORM.

In one segment of work, we developed a gamma background estimation model using a Long-short term memory (LSTM) network for one-step CPS time series prediction [4]. The LSTM model was validated with two data sets of measurements from two independent NaI detectors positioned on a mobile platform. The data sets contained background radiation only and no orphan isotope sources. The LSTM model was constructed and tested using data from one of the detectors. Performance of the LSTM model was validate through one-step prediction of CPS time series of *another* NaI detector *without re-training*. This approach allows to create a *digital twin* for nuclear background estimation. Using LSTM, it could be possible to detect a source through subtraction of the estimated counts from the measured background.

In another segment of work, we investigated detection of gamma emitting sources in the presence of complex background using unsupervised machine learning. Spectral lines of isotopes are difficult to observe in one-second measurements. Averaging over the entire measurement campaign data set reveals spectral lines of most common background isotopes. Spectral lines of orphan sources, which might appear only in a few measurements during the campaign, will be washed out if averaging is performed over the entire measurement data set. The approach we have explored consists of extracting one-second measurements containing weak spectral features through data clustering. Averaging one-second spectra in a cluster should reveal the presence of anomaly sources. We created two ML models using K-means clustering and Neural Network Self-organizing Map (SOM) [5,6]. Performance of these ML models was benchmarked using search data. One data set contained ^{137}Cs source, and another dataset contained ^{131}I source.

2. Development of Digital Twin of Gamma Background Radiation with LSTM

Gamma radiation background measured during environmental screening with a moving detector exhibits significant fluctuation with time. We have developed a *digital twin* of gamma radiation background using LSTM model. The LSTM model was developed and validated using background gamma spectra obtained with two independent NaI detectors-spectrometers. Both datasets were recorded at the same time. One detector was positioned on the left side and the other on the right side of a moving vehicle. Each NaI detector measured gamma counts in 1024 channels corresponding to the energy range from 0 to 3000keV. Each detector recorded 12207 one-second spectra. Figure 3 shows the time series of energy-integrated counts per second (CPS) for both the left and right detector during the data collection. One can observe from the two panels in Figure 8 is that the data measured with two detectors is not identical, but highly correlated. The left detector readings are slightly higher than those of the right detector.

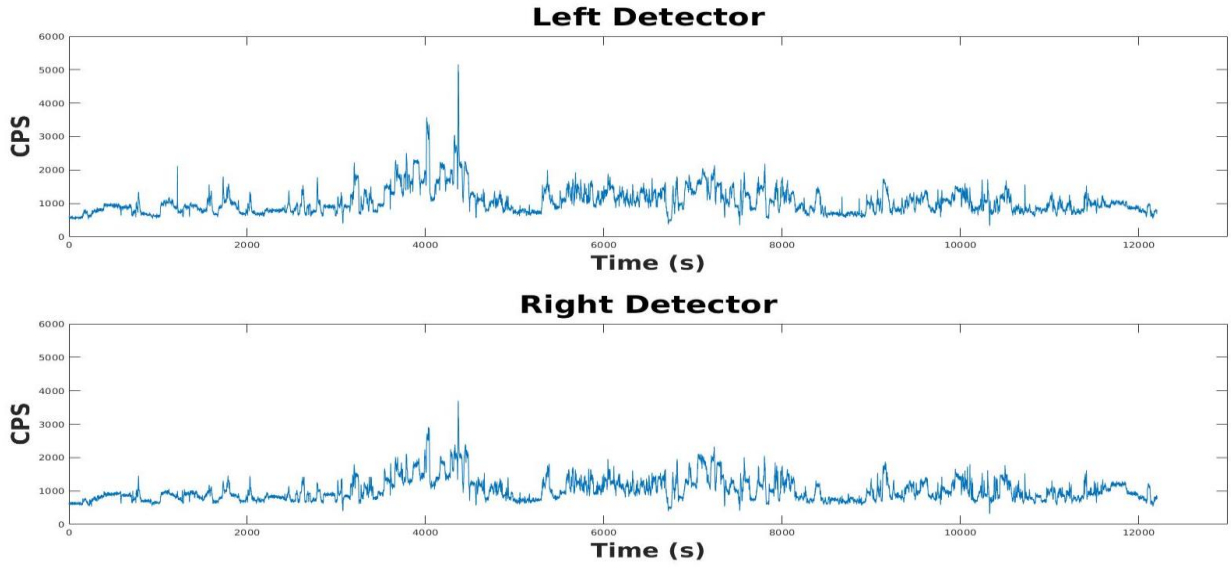

Figure 3 – CPS time series of left and right NaI detectors concurrently measuring gamma background.

LSTM networks have been shown to be useful for learning sequences containing longer term patterns of unknown length, due to their ability to maintain long term memory. Stacking recurrent hidden layers in such networks also enables the learning of higher level temporal features, for faster learning with sparse representations. Thus making an LSTM network suitable for time-series data such as nuclear background spectra. In this work, we created LSTM model using data from the *left detector*, and used this LSTM model for one-step prediction of the time series of *right detector*.

Our model was created using MATLAB Deep Learning Toolbox software, where we normalized the data by the maximum count of the dataset, and broke up the dataset into two parts, training and test data. The training dataset contained 90% contiguous data and the last 10% for

testing the model. The LSTM network input data is 1024 features and 1024 responses for each channel in the detector with 200 LSTM hidden layers. The LSTM network was trained for a maximum of 50 epochs or until the loss function is consistently below 0.1 to avoid over training the network. Root mean square error (RMSE) in estimates is calculated as:

$$RMSE = \sqrt{\prod_{i=1}^{n} \frac{(\widehat{y_i} - y_i)^2}{n}} \qquad (1)$$

where $\hat{y}_i$ are the predicted values, y_i are observed values, and n is the number of observations.

2.1. Development and testing of LSTM model with left detector background gamma measurements

Figure 4 shows the left NaI detector CPS time series, which are broken into training data colored blue (90% of data), test data colored green, and the one-step prediction colored orange.

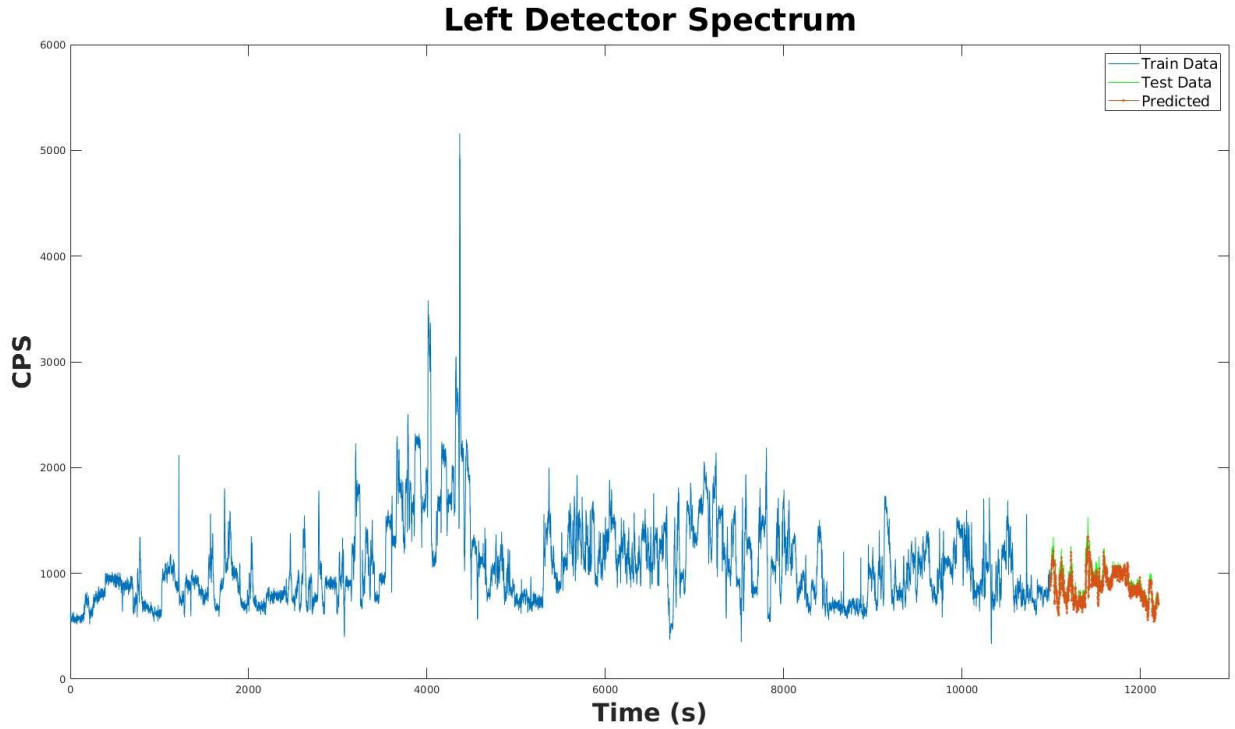

Figure 4 – Training and prediction of left NaI detector CPS time series with LSTM. Training data is colored in blue, test data in green, and predicted in orange.

Figure 5 shows the zoomed-in test/predicted segment of the time series in Figure 4. The color scheme is the same as in Figure 4.

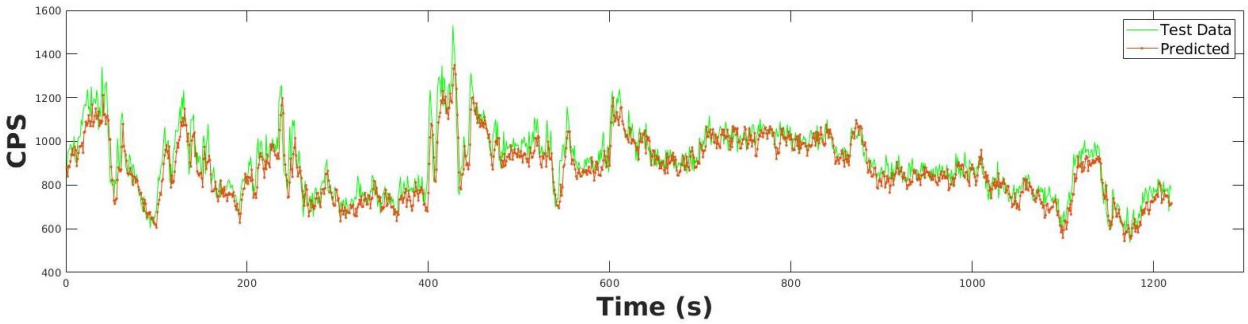

Figure 5 – Zoomed-in test/predicted data segment of the left NaI detector CPS time series.

The error in one-step prediction with LSTM is plotted in Figure 6. We obtain RMSE = 687.

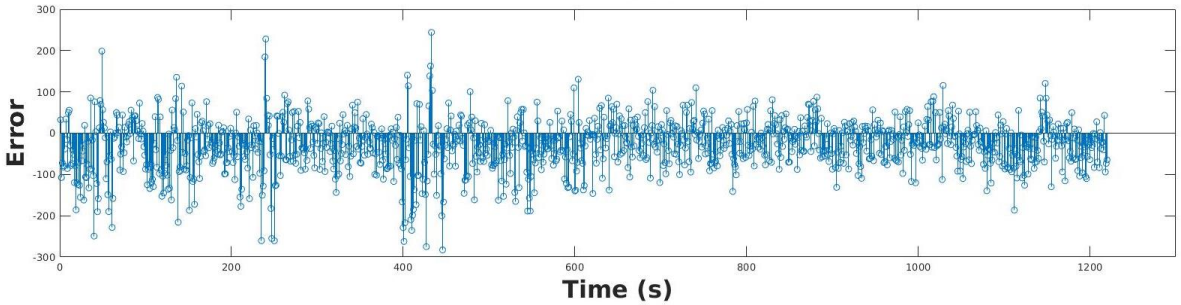

Figure 6 – Error in one-step prediction with LSTM for the right detector. RMSE = 687.

2.2. Validation of LSTM model with right detector background gamma measurements

To test performance of the LSTM model digital twin developed using the *left detector* training data, we applied the LSTM model to predict previously unseen data in the *right detector* dataset. The test consists of one-step prediction, where the input at time *t* is a one-second spectrum with 1024 features (detector channels), and the LSTM model predicts the next time step *t* + 1. Figure 7 shows the prediction on the entire 12207 measurements in the right detector data set. The observed data colored in blue, and the predicted output from the LSTM network colored in orange.

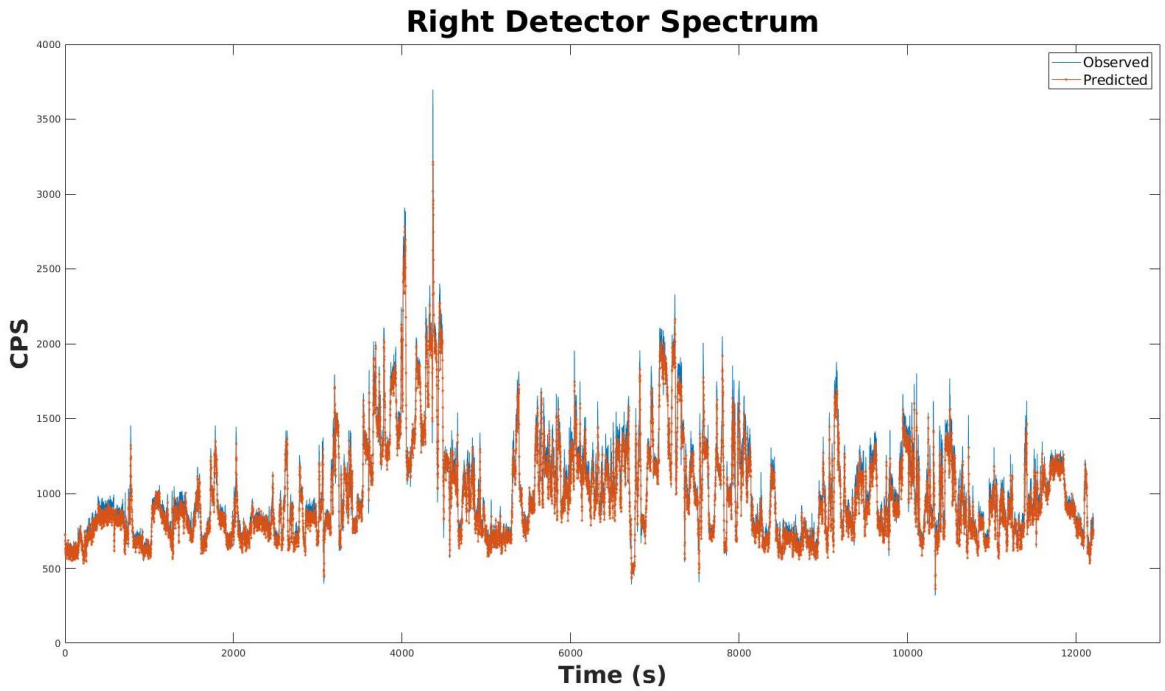

Figure 7 – One-step prediction of right detector CPS time series with LSTM model developed using training data from the left detector.

Zoomed-in segment of the data in Figure 7 between time points 4000 and 5000 is shown in Figure 8. As can be seen, the LSTM model closely follows the observed values with the largest error when the CPS increases suddenly at approximately 4380s.

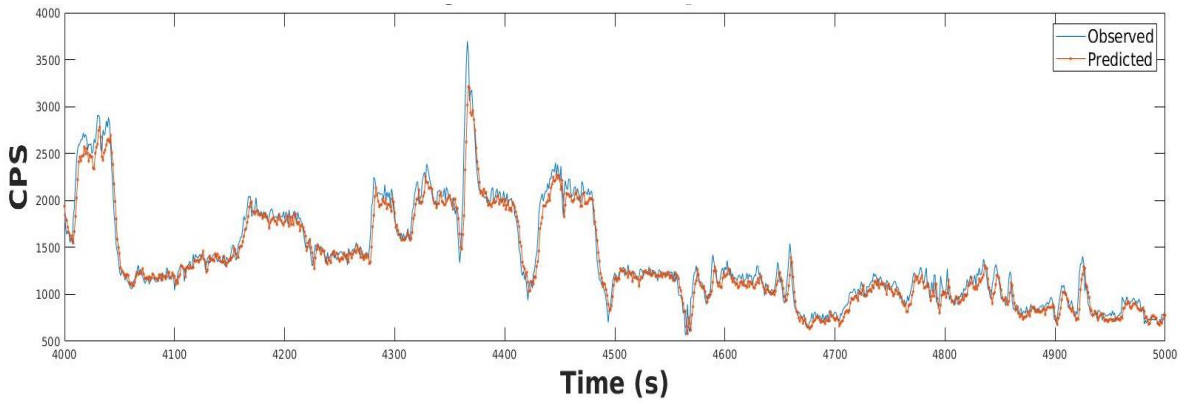

Figure 8 – Zoomed-in (measurements 4000 to 5000) one-step prediction of right detector CPS time series with LSTM model developed using training data from the left detector.

The error in estimates in Figure 8 is plotted in Figure 9. We obtain RMSE = 1192. This number is comparable to RMSE value obtained in Figure 6.

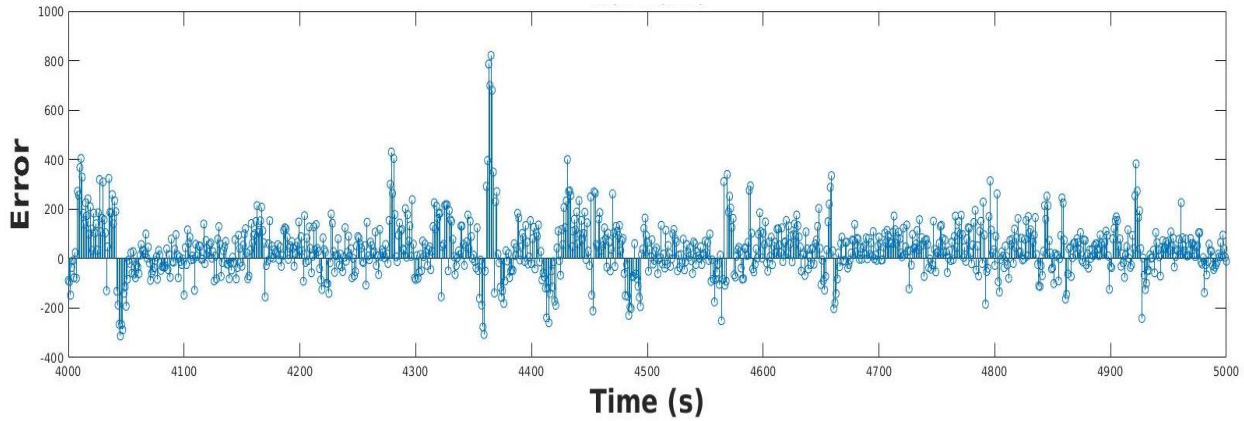

Figure 9 – Error in one-step prediction of the right detector using LSTM developed with training data from the left detector. RMSE = 1192.

3. Gamma Source Detection with Clustering Algorithms

One-second spectra acquired with a moving platform show weak spectral signatures of isotopic sources. Averaging over multiple measurements will increase the S/N of isotopic spectral lines, which would allow for unambiguous detection and identification. However, the key decision consists of choosing the segment of measurement data for averaging. For example, if measurement is performed over all data taken during several-hour environmental screening campaign, spectra of orphan sources is washed out. Signal from an orphan source are most likely to be found in a small subset of total measurements. On the other hand, all measurements contain signals due to isotopes found in NORM. As an illustration, in Figure 10 we plot the spectrum averaged over search time in the data set of 4265 one-second gamma spectrum measurements performed with a moving NaI detector. The measurement set containing 96 one-second spectra of ^{137}Cs isotope, which is not part of the natural background. In the plot of Figure 10 of time-averaged number of gamma counts $<N_\gamma>_T$ as a function of energy E, the peaks are due to NORM. The peak at 662 keV corresponding to ^{137}Cs isotope is not visible.

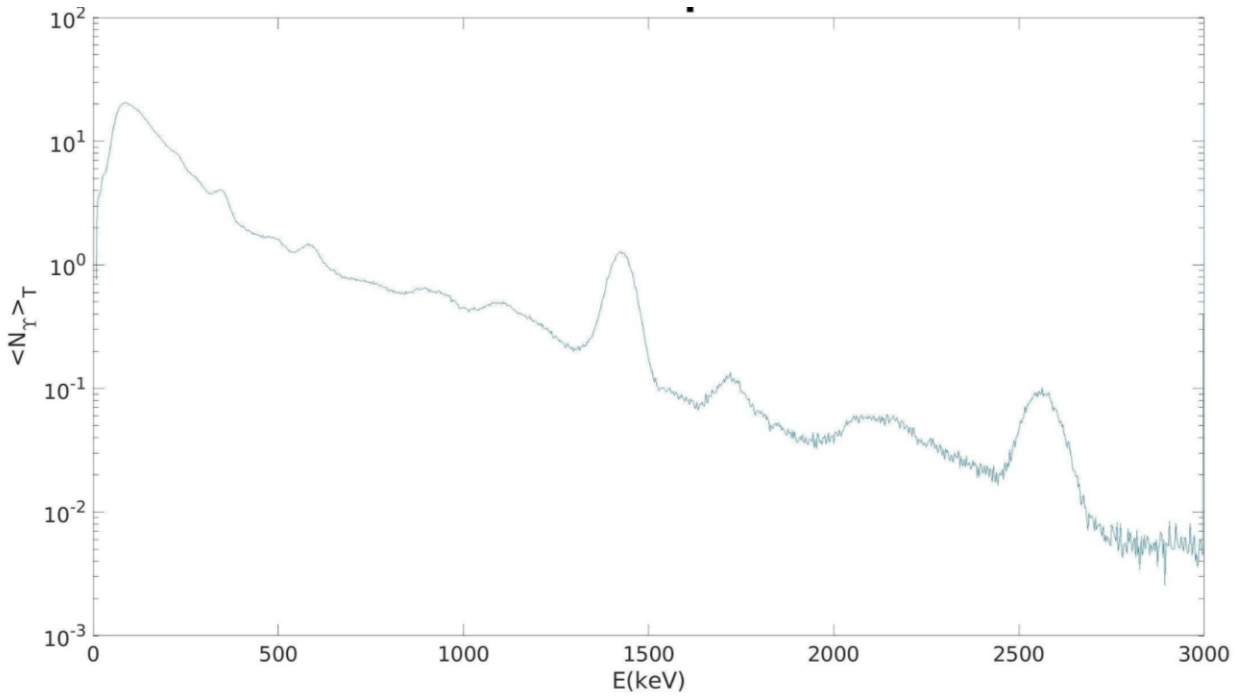

Figure 10 – Gamma spectrum in the energy range 0 – 3000keV averaged over 4265 total measurements. The line of ^{137}Cs isotope at 662keV is washed out.

In our approach, we select a subset of total measurements for averaging using two Unsupervised Learning clustering analysis techniques called Neural Network SOMs and K-means clustering. Clustering is one of the most common exploratory data analysis techniques used to get an intuition about the structure of the data. The method can assist in identifying subgroups in the data such that data points in the same subgroup or cluster are very similar while data points in

different clusters are very different. Clustering analysis can be done on the basis of features, where we try to find clusters of samples based on its feature

Clustering algorithms were used to detect orphan ^{137}Cs and ^{131}I isotopes. The first dataset contained 4265 one-second spectra from a NaI scintillation detector, including 96 one-second spectra of ^{137}Cs source. The second dataset contained 5827 one-second spectra from a NaI scintillation detector, including 89 one-second spectra of ^{131}I source. Both datasets contained 1024 channels ranging from 0 to 3000keV. The models were created using MATLAB Deep Learning Toolbox software. We performed a normalization procedure on both datasets so that the largest value in each spectra was scaled to unity. This normalization procedure ensures that clustering would not be sensitive to fluctuation in total counts. Once the datasets were clustered, we then determined its precision, recall, and F_1 score to evaluate the model with the following equations:

$$Precision = \frac{tp}{tp + fp} \quad (2)$$

$$Recall = \frac{tp}{tp + fn} \quad (3)$$

$$F_1 = 2 * \frac{precision * recall}{precision + recall} \quad (4)$$

where t_p is true positives, f_p is false positives, and f_n is false negatives. For K-means clustering, due to the varying centroids, we took an average of the precision and recall between ten trials, which we then used to create the average F_1 score

3.1. K-means clustering algorithm

K-means algorithm is an interactive algorithm that tries to partition or separate the dataset into sections or K clusters. Each data point will belong to only one cluster and the algorithm tries to make the intra-cluster data point as similar as possible while also keeping the clusters as different as possible. It assigns data points to a cluster such that the sum of the squared distance between the data points and the cluster's centroid is at the minimum. Therefore, for each model we will need to specify the number of clusters K, initialize centroids by shuffling the dataset, then randomly selecting the centroids for each K, iterate until there is no change in the centroid, and compute the sum of the squared distance between data points and all centroids.

3.1.1. K-means clustering of dataset with ^{137}Cs source

Applying the K-means clustering algorithm to the dataset containing ^{137}Cs source, we used K = 11 for a total of 11 clusters. Each iteration of K-means was also able to visualize ^{137}Cs in one of the clusters with the number of predictions ranging from 82 - 115 one-second spectra, where the original dataset had 96 one-second spectra of ^{137}Cs source. Averaged gamma spectrum of K-means cluster with 84 one-second spectra, is plotted in Figure 11 Averaging of one-second spectra in the anomaly cluster reveals ^{137}Cs 662keV line.

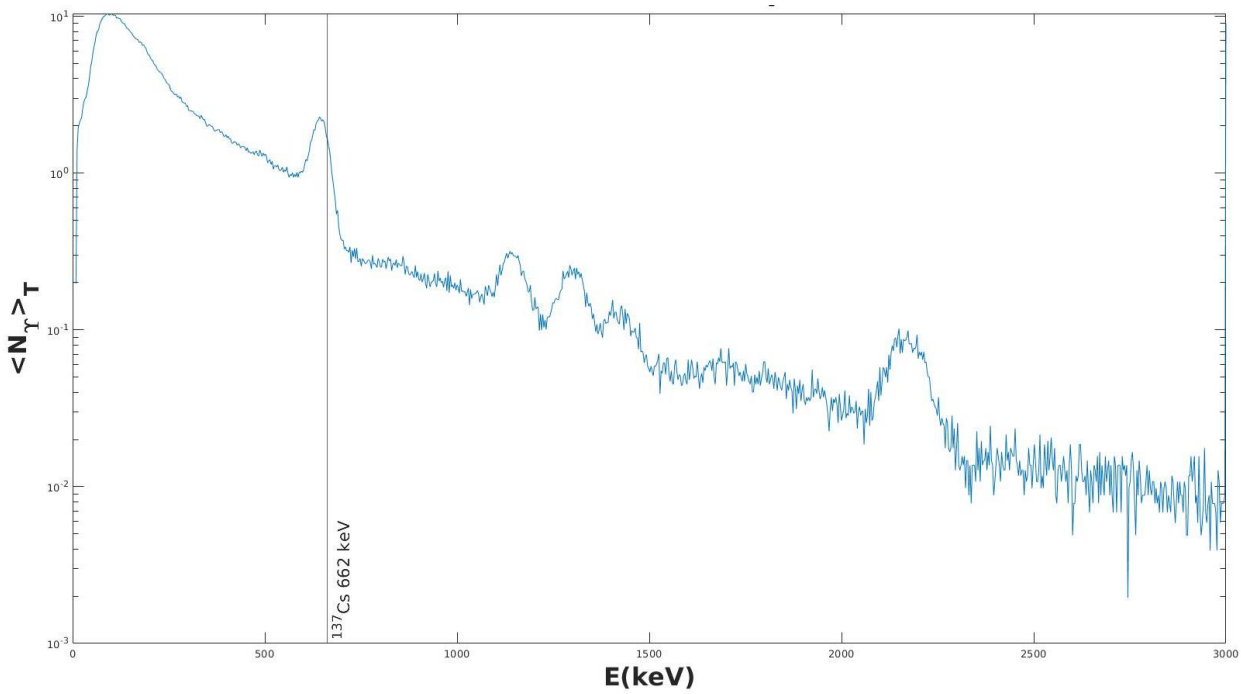

Figure 11 – Averaged gamma spectrum of K-means anomaly cluster with 84 one-second spectra. Averaging of one-second spectra in the anomaly cluster reveals ^{137}Cs line.

Average results for K-means clustering of the data set with ^{137}Cs source are shown in Table 1. The average F_1 score is 85.28%.

Table 1 – Precision, Recall, and F1 score for K-means clustering of data with ^{137}Cs source

Samples	96
# of trials	10
Predicted	82 - 115
Average Precision	82.57%
Average Recall	81.67%
Average F_1 score	**85.28%**

3.1.2. K-mean clustering of dataset with ^{131}I source

Applying the K-means clustering algorithm to the dataset containing ^{131}I isotope, we used K = 3 for a total of 3 clusters. Each iteration of K-means was also able to visualize ^{131}I in one of the clusters with the number of predictions ranging from 91 - 92 one-second spectra, where the original dataset had 89 one-second spectra of ^{131}I. Averaged gamma spectrum of K-means cluster with 91

one-second spectra, is plotted in Figure 12. Averaging of one-second spectra in the anomaly cluster reveals ^{131}I isotope 364keV line.

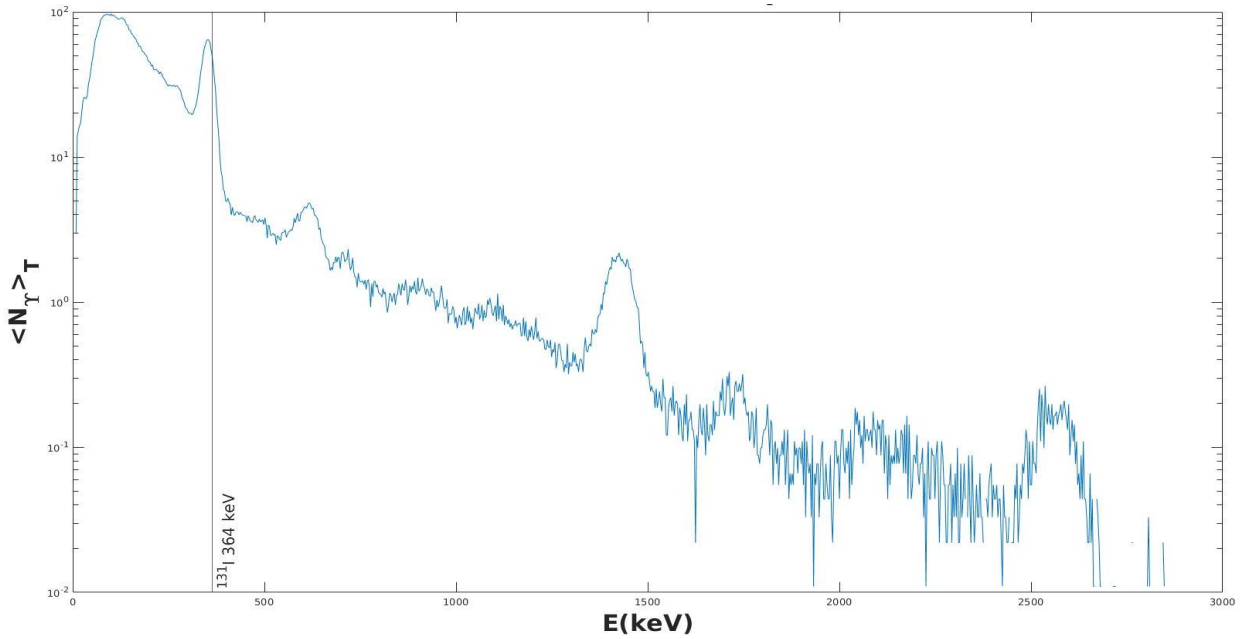

Figure 12 – Averaged spectrum on K-means anomaly cluster with 91 one-second spectra. Averaging of one-second spectra in the anomaly cluster reveals ^{131}I line.

Average results for K-means clustering of the data set containing ^{131}I source are shown in Table 2. The average F_1 score is 91.11%.

Table 2 – Precision, Recall and F_1 score for SOM for ^{131}I source detection.

Samples	89
# of trials	10
Predicted	91 - 92
Average Precision	91.11%
Average Recall	91.13%
Average F_1 score	**91.11%**

3.2. Neural network self-organizing map (SOM) clustering algorithm

A self-organizing map (SOM) is a type of artificial neural network (ANN) that uses unsupervised learning to produce a low dimensional, discretized representation of the input space of the training

samples, called a map, and is therefore a method to do dimensionality reduction. With the use of competitive learning, as opposed to backpropagation like other ANNs, a SOM can use a neighborhood function to preserve the topological properties of the input space. The algorithm begins by first initializing each node's weight, then a vector is chosen at random from the set of training data where each node is examined to calculate which one's weights are most like the input vector. The winning node is known as the Best Matching Unit (BMU), which is a technique that calculates the distance from each weight to the sample vector, by running through all weight vectors. The weight with the shortest distance is the winner. The winning weight is rewarded with becoming more like the sample vector. The neighbors also become more like the sample vector. The closer a node is to the BMU, the more its weights get altered and the farther away the neighbor is from the BMU, the less it learns. This process then repeats for every input vector in the dataset for N epochs.

3.2.1. SOM clustering of dataset with ^{137}Cs source

For applying the SOM network to the dataset containing ^{137}Cs source, we used a map size of 3 and trained the network for 200 epochs which resulted in a total of 9 clusters. Plotting of all the partitions revealed that one of the clusters could visualize the peak at 662 keV for ^{137}Cs, as shown in Figure 13. The model had placed 101 one-second spectra into the same cluster while the original dataset had 96 one-second spectra of the ^{137}Cs source. Averaging of one-second spectra in the anomaly cluster reveals ^{137}Cs 662keV line.

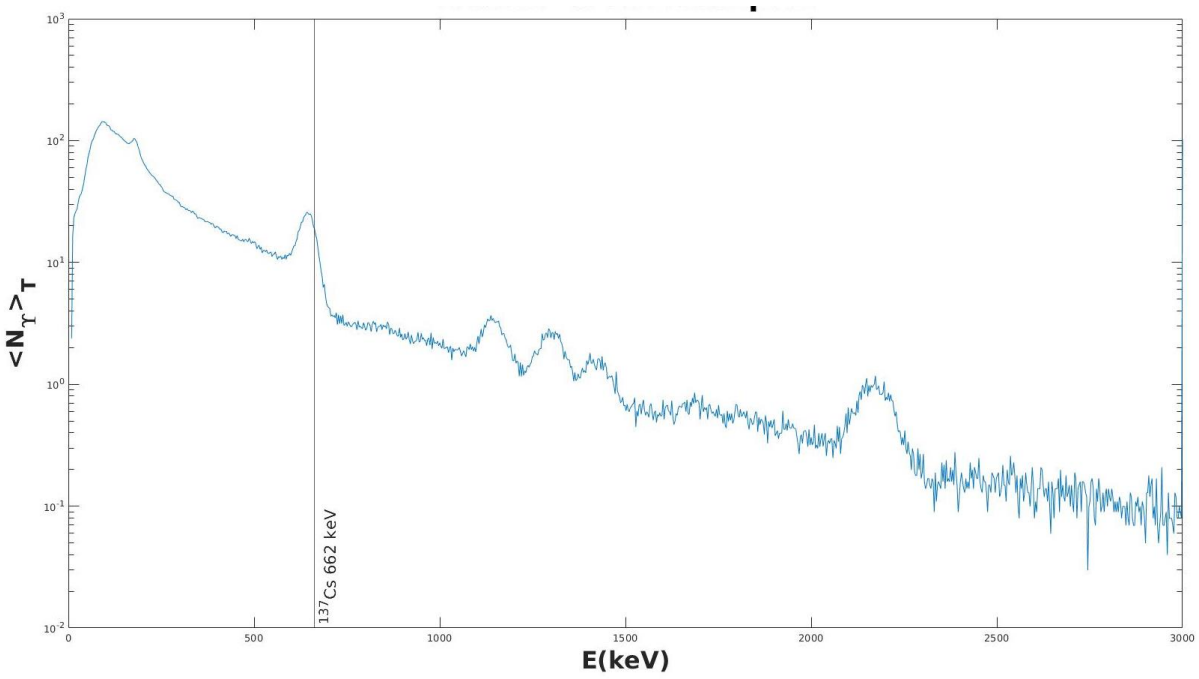

Figure 13 – Averaged gamma spectrum of SOM anomaly cluster with 101 one-second spectra. Averaging of one-second spectra in the anomaly cluster reveals ^{137}Cs line.

Table 3 shows the calculated precision, recall, and F_1 score of the SOM model for the dataset containing ^{137}Cs source. The F_1 score is 85.28%.

Table 3 – Precision, Recall and F_1 score for SOM for ^{137}Cs source detection.

Samples	96
Predicated	101
True Positives	84
False Negatives	12
False Positives	17
Precision	83.17%
Recall	87.50%
F_1 score	**85.28%**

3.2.2. SOM clustering of dataset with ^{131}I source

For applying the SOM network to the dataset containing ^{131}I isotope, we used a map size of 2, and trained the network for 200 epochs which resulted in a total of 4 clusters. Plotting of all the partitions revealed that one of the clusters could visualize the peak at 364 keV for ^{131}I as shown in Figure 14. The model had placed 91 one-second spectra into the same cluster, while the original dataset had 89 one-second spectra of the ^{131}I source. Averaging of one-second spectra in the anomaly cluster reveals the ^{131}I isotope 364keV line.

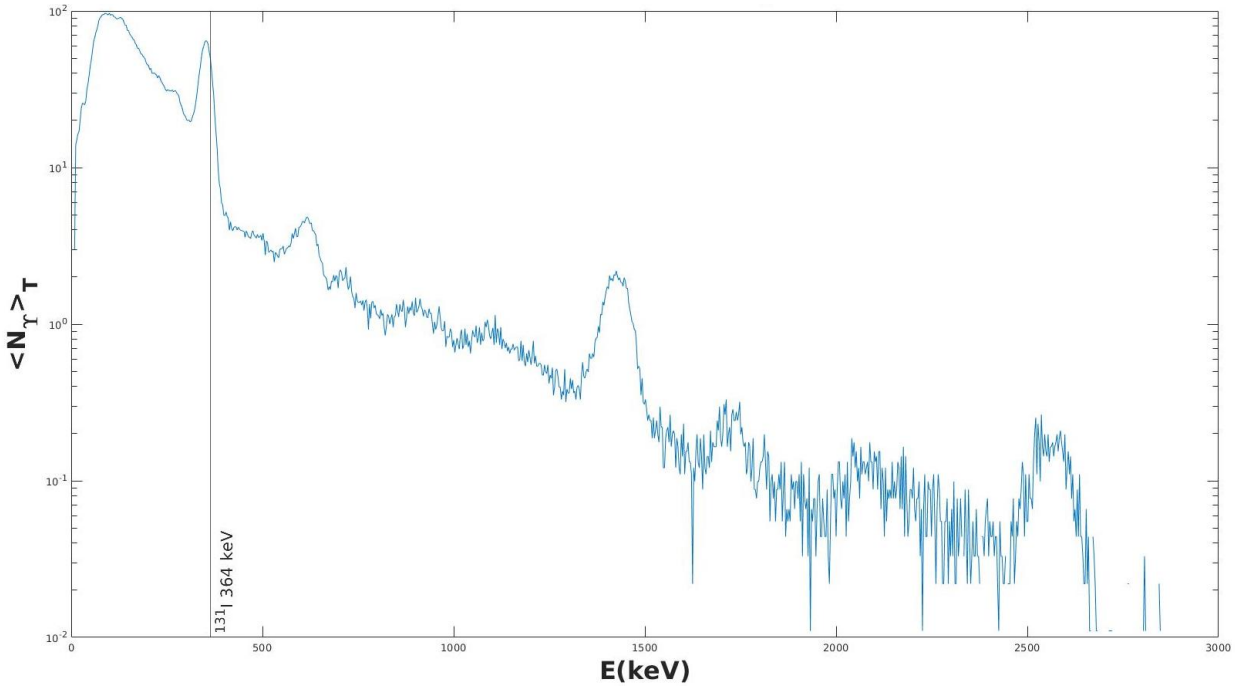

Figure 14 – Averaged gamma spectrum of SOM cluster with 91 one-second spectra. Averaging of one-second spectra in the anomaly cluster reveals the ^{131}I line.

Table 4 shows the precision, recall, and F_1 score of the SOM model for the data set containing ^{131}I source. The F_1 score is 91.23%.

Table 4 – Precision, Recall and F_1 score for SOM for ^{131}I detection.

Samples	89
Predicated	91
True Positives	82
False Negatives	7
False Positives	9
Precision	90.11%
Recall	92.36%
F_1 score	**91.23%**

3.3. Summary of Clustering Results

The results have shown that both algorithms can successfully cluster both dataset sources into a single cluster with an accuracy of greater than 82%. Comparing both algorithms together, Neural Network SOMs outperform K-means clustering in both the F_1 scores metric for the datasets, and in the algorithm run time metric. Table 5 shows performance benchmarking results of the two algorithms for two different data sets.

Table 5 – Benchmarking of clustering algorithms performance

Algorithm	**^{137}Cs Data Set (F_1 score)**	**^{131}I Data Set (F_1 score)**	**Run time**
Neural Network SOM	85.28%	91.23%	~0.1 seconds
K-means clustering	82.11%	91.11%	~0.5 seconds

4. Conclusions

We have investigated several unsupervised machine learning algorithms for analysis of gamma spectrum measurements obtained in environmental wide are screening with a moving NaI detector-spectrometer. In our work in Background Estimation, we developed a model using LSTM for the background prediction in near real-time analysis. Using one-step prediction the LSTM model predicts the next time step on the test data and on unseen data from the right detector. Preliminary results show that LSTMs can be an efficient method of background prediction but need to be benchmarked. For future work, we will apply the background estimator to a dataset with a nuclear source. The model should predict the next time step minus the nuclear source data therefore we could subtract the observed data minus the predicted data to assist in nuclear source detection.

For the work on weak anomaly and nuisance detection, we developed K-means clustering and neural network self-organizing maps (SOM) algorithms. The validation study consisted of two data sets of spectra measured in one-second intervals with a Sodium Iodide detector. The first dataset with over 4000 spectra consisted mostly of urban background measurements and approximately 90 measurements of ^{137}Cs. The second dataset consisted of over 5000 spectra mostly of urban background and approximately 90 measurements of ^{131}I. Using clustering analysis, we observed that a majority of spectra containing nuclear source signals clustered away from the background, producing point-like clusters when visualizing in search-time averaged number of gamma counts. One cluster in both datasets contained spectra with strong ^{137}Cs peaks and ^{131}I in over 85% of the clustered samples. The other clusters contained no visible peaks of the nuclear source in their spectra.

Development of a robust clustering technique for detection of sources will require further algorithm optimization sensitivity of cluster feature identification in the spectrum to the detector response function of NaI. This would provide a better understanding of the limits of the source detection capability of cluster based techniques. It is expected that cluster performance will depend on such factors as source spectrum and signal strength, background isotopic composition and variability with time. Such studies will also provide an indication if the detector spectral channels can be ranked in order of importance for cluster analysis. Channels with least importance could be excluded from data to reduce its size, and hence increase the speed of analysis.

References

1. Weinstein, M., Heifetz, A., & Klann, R. (2014). Detection of nuclear sources in search survey using dynamic quantum clustering of gamma-ray spectral data. The European Physical Journal Plus, 129(11), 239.
2. Alamaniotis, M., Heifetz, A., Raptis, A. C., & Tsoukalas, L. H. (2013). Fuzzy-logic radioisotope identifier for gamma spectroscopy in source search. IEEE Transactions on Nuclear Science, 60(4), 3014-3024.
3. Bai, E. W., Heifetz, A., Raptis, P., Dasgupta, S., & Mudumbai, R. (2015). Maximum likelihood localization of radioactive sources against a highly fluctuating background. IEEE Transactions on Nuclear Science, 62(6), 3274-3282.
4. Malhotra, P., Vig, L., Shroff, G., & Agarwal, P. (2015, April). Long short term memory networks for anomaly detection in time series. In Proceedings (Vol. 89, pp. 89-94). Presses universitaires de Louvain.
5. Kanungo, T., Mount, D. M., Netanyahu, N. S., Piatko, C. D., Silverman, R., & Wu, A. Y. (2002). An efficient k-means clustering algorithm: Analysis and implementation. IEEE transactions on pattern analysis and machine intelligence, 24(7), 881-892.
6. Vesanto, J., & Alhoniemi, E. (2000). Clustering of the self-organizing map. IEEE Transactions on neural networks, 11(3), 586-600.

Nuclear Science and Engineering (NSE) Division
Argonne National Laboratory
9700 South Cass Avenue, Bldg. 208
Argonne, IL 60439

www.anl.gov